Degenerate ground-state lattices of membrane inclusions

K. S. Kim,[1] Tom Chou,[2,*] and Joseph Rudnick[3]
[1]*Lawrence Livermore National Laboratory, Livermore, California 94550, USA*
[2]*Departments of Biomathematics and Mathematics, UCLA, Los Angeles, California 90095-1766, USA*
[3]*Department of Physics and Astronomy, UCLA, Los Angeles, California 90095, USA*
(Received 13 October 2007; revised manuscript received 19 January 2008; published 7 July 2008)

Particles that are embedded in fluid membranes or plates can induce bending if they impose a nonzero angle of contact. This bending mediates complicated effective particle-particle interactions. In the absence of tension, these interactions are nonpairwise additive and can result in clusters of particles with specific configurations that give rise to zero total membrane bending energy. Here, we consider an infinite periodic lattice of such membrane inclusions. Upon summing the nonpairwise interactions within a regular lattice, we find an unexpected infinite number of periodic lattices that preserve zero membrane bending energy. Elliptically shaped membrane inclusions further increase the phase space of this degeneracy.

DOI: 10.1103/PhysRevE.78.011401 PACS number(s): 82.70.−y, 87.16.D−, 87.85.J−, 05.70.Np

I. INTRODUCTION

Consider embedding particles in a thin bendable membrane. If the membrane contacts the particles at a fixed angle γ, and is asymptotically flat far away from the inclusion, it will be bent (see Fig. 1). It has been shown that when many particles are embedded in the membrane plate, the total deformation induces nontrivial nonpairwise additive interactions among the inclusions [1]. Furthermore, if the particles are mobile within the membrane surface (such as the case for fluid membranes), they will reach mechanical equilibrium by rearranging into configurations that minimize the total bending energy.

One physical example of inclusions embedded in fluid membranes are integral membrane proteins embedded in lipid bilayers. These proteins mediate biological functions such as transport and cellular adhesion [2]. The spatial organization of membrane proteins may also play an important part in cell signaling [3,4]. In previous theoretical studies, protein-protein interactions mediated by large deformations of lipid membranes were treated within plate theory [5,6], where strains in the plane of the plate are negligible compared to its transverse displacement [7]. Similarly, membrane-mediated interactions among a large number of inclusions have been studied within the small membrane deformation limit [1,8–10,12,13,15]. It was found that in the absence of surface tension, the energy cost of adding an additional inclusion arose from the local Gaussian curvature generated by the deformation induced by all the other embedded particles. Although the local scalar curvature field is additive in the number of inclusions, the bending energy associated with inserting an additional protein is proportional to the square of the local Gaussian curvature, which is the square magnitude of the complex curvature scalar. This "square of sums" structure results in nonpairwise interactions among the membrane proteins. One feature of these nonpairwise interactions is the admittance of small clusters with "magic numbers" of inclusions in specific configurations that completely cancel the total membrane bending energy. The local structures of these lattices were found to be nearly triangular or square [1].

In this paper, we consider the total bending energy of infinite, doubly periodic lattices. These minimum-energy lattices are somewhat analogous to those found by taking the infinite size limits of the previously found zero-energy clusters. Although the main motivation for studying this type of system arises from a desire to understand membrane protein organization, in this mathematical treatment, we neglect molecular and biochemical details associated with realistic integral membrane protein models. Nonetheless, our analysis of minimum-energy lattices in such a multibody interacting system may be relevant to *in situ* crystallization of integral membrane proteins [14]. After first reviewing the energy of multiple embedded inclusions, we compute lattice energies by summing over an asymptotically infinite regular array of membrane-embedded inclusions. Surprisingly, we find that not only are zero-energy configurations preserved, but that an infinite number of distinct zero-energy periodic lattices arise.

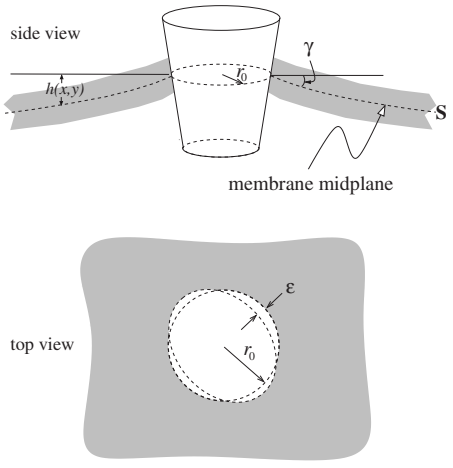

FIG. 1. Membrane with an embedded inclusion of radius r_0 and ellipticity ε. The inclusion imposes a contact angle γ at its boundary with the membrane midplane.

*tomchou@ucla.edu

II. MULTIBODY INTERACTIONS

Equilibrium configurations of a bendable membrane are typically found by minimizing the Canham-Helfrich bending energy [16]

$$\mathcal{H}_{\text{mem}} = \frac{\kappa}{2}\oint K^2(\mathbf{S})d\mathbf{S}, \tag{1}$$

where $\mathbf{S}$ is the surface element, κ is the membrane bending rigidity, and $K(\mathbf{S})$ is the local mean curvature. For our analysis, we neglect tension in the membrane. Descriptions of membrane deformations using the Helfrich free energy are equivalent to treating the membrane as an ideal elastic plate where strains in the plane of the plate are negligible compared to the transverse displacements [7]. Mechanical equilibrium is described by minimizing Eq. (1) with respect to membrane configurations, in the presence of constraints such as boundary conditions. One such constraint is the specification of the contact angle γ around a contact curve defining the intersection of a conical inclusion and the membrane (Fig. 1).

In previous work [1,10], the bending-mediated interaction energies were derived in the limit where inclusion separations were much greater than their size. The derivation makes use of the solution to the biharmonic equation $\Delta^2 h(x,y)=0$ obtained from functionally minimizing $\mathcal{H}_{\text{mem}}$ in the small $h(x,y)$ (out-of-plane deformation) limit. The solution for a single isolated inclusion, satisfying the contact angle at the contact line $r=r_0$, and being asymptotically flat far away, is $h(r)=-\gamma \ln(r/r_0)$. However, in the presence of other inclusions the general solution will no longer be axisymmetric and also contains additional powers in the distance r from the reference point at which an additional inclusion will be added. Upon asymptotically matching the local deformations induced by an additional inclusion with the general far-field solutions, the total deformation is found in terms of elements of the curvature tensor. When this deformation is substituted into $\mathcal{H}_{\text{mem}}$, the resulting bending energy cost of embedding an additional inclusion at the origin is

$$E_1 = 4\pi\kappa|\eta|^2 \tag{2}$$

where $|\eta|^2$ is the local Gaussian curvature at the origin prior to insertion. If this Gaussian curvature is caused by the presence of another protein a distance r away, the complex curvature field can be expressed as $\eta=\gamma r_0^2/z^2$, where $z=x+iy$, $r^2=x^2+y^2$. When there are many particles, the scalar curvature field is additive in the number of other inclusions at positions z_i generating the local deformation $\eta=\Sigma_{i=2}^{N}\gamma r_0^2 z_i^{-2}$. However, since the bending energy is proportional to $|\eta|^2$, the interaction energies are nonadditive with respect to the inclusions. From Eq. (2), the energy of inserting a protein in the deformation field of $N-1$ others is thus

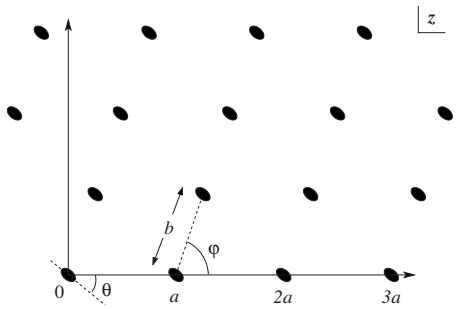

FIG. 2. A schematic of the doubly periodic, infinite lattices (defined in the complex plane z) formed by regularly spaced, elliptically shaped membrane inclusions. The basis vectors have angle φ between them and have magnitudes a and b. The angle between the long axis of the jth elliptical inclusion and one of the basis vectors is denoted θ_j.

$$E_1 = 4\pi\kappa|\eta|^2 = E_0\left|\sum_{i=2}^{N}\frac{r_0^2}{z_i^2}\right|^2, \tag{3}$$

where $E_0 \equiv 4\pi\kappa\gamma^2$. The total interaction energy of a collection of N identical, circular inclusions embedded in a membrane of bending rigidity κ is thus [1,10]

$$E_N = E_0\sum_{j=1}^{N}\left|\sum_{i\neq j}\frac{r_0^2}{(z_i-z_j)^2}\right|^2. \tag{4}$$

As shown in [1] and [10], the interaction energy for elliptically shaped (with ellipticity ε, inclusions can be similarly derived. A lattice of elliptically shaped inclusions is depicted in Fig. 2. If the jth inclusion has an angle θ_j between its major axis and an arbitrary reference axis, the bending-mediated interaction energy takes the form

$$E_N = E_0\sum_{j=1}^{N}\left|\sum_{i\neq j}\frac{r_0^2}{(z_i-z_j)^2} - \frac{\varepsilon}{2}e^{-2i\theta_j}\right|^2. \tag{5}$$

III. PERIODIC LATTICES

We now search for minimum-energy lattices by summing the interaction energies for an infinite periodic array of inclusions. We normalize the distances with respect to the lattice spacing a along one basis vector direction, $(z\rightarrow z/a)$. If the two-dimensional array of inclusions is perfectly periodic, we can express the position of the ith particle by

$$z_i = m_i + n_i b e^{i\varphi}, \tag{6}$$

where m_i is the normalized distance of the ith inclusion along the real axis and n_i is the number of units along the other lattice vector. For example, perfect square (triangular) lattices are defined by $b=1$ and $\varphi=\pi/2$ $(\pi/3)$.

Upon substitution of Eq. (6) into Eq. (5), and using the Poisson summation formula [17],

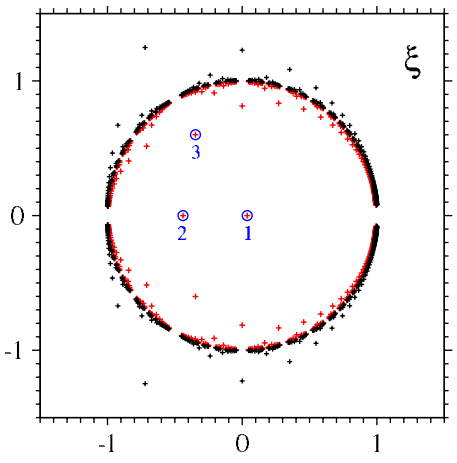

FIG. 3. (Color online) The first 250 roots of $|S(\xi)|$ (with amplitude $|\xi_i|<1$, increasing with index i) and their complex conjugates and inverses. All the inverses $1/\xi_i, 1/\xi_i^*$ are shown except for those of the two real roots nearest the origin. Three representative roots are circled.

$$\sum_{m_i=-\sqrt{N}/2}^{+\sqrt{N}/2} [(m_i - m_j) + (n_i - n_j)be^{i\varphi}]^{-2} = \begin{cases} \frac{\pi^2}{3} + o(1/\sqrt{N}), & n_i = n_j, \\ \pi^2 \csc^2\{\pi[m_j - (n_i - n_j)be^{i\varphi}]\}, & n_i \neq n_j, \end{cases} \quad (7)$$

we find a total membrane bending energy of the form

$$E = 64\pi^4 E_0 \left(\frac{r_0}{a}\right)^4 \sum_{j=1}^{N} \left| S(\xi) + \varepsilon \left(\frac{a}{4\pi r_0}\right)^2 e^{-2i\theta_j} \right|^2, \quad (8)$$

where

$$\xi \equiv \exp(2\pi i b e^{i\varphi}), \quad (9)$$

and

$$S(\xi) \equiv -\frac{1}{24} + \sum_{p=1}^{\infty} \frac{\xi^p}{(\xi^p - 1)^2} = -\frac{1}{24} + \sum_{p=1}^{\infty} \sum_{k=1}^{\infty} k\xi^{pk} \quad \text{for } |\xi| < 1. \quad (10)$$

First consider circular inclusions with $\varepsilon=0$. Since $S(\xi)$ is independent of the particle index j, the lattice parameters for circular inclusions are simply determined from minimization of the energy density $|S(\xi)|^2$. For circular inclusions, the energy is of the form $E \propto A/a^4$, and at each of the infinite minima, $A=0$. Thus, for a given minimum, the lattice bending energy vanishes, rendering the lattice invariant to dilations. Additional interaction terms and an external chemical potential would be required to tune the lattice constants and fix the overall inclusion density.

Since $S(\xi)=S(1/\xi)$, the roots ξ_i of $|S(\xi)|$ come in quadruples $(\xi_i, \xi_i^*, 1/\xi_i, 1/\xi_i^*)$. Therefore, it suffices to consider roots $|\xi_i|<1$ and use for computation, the second, polynomial form in Eq. (10). The first 250 roots, ξ and ξ^*, were

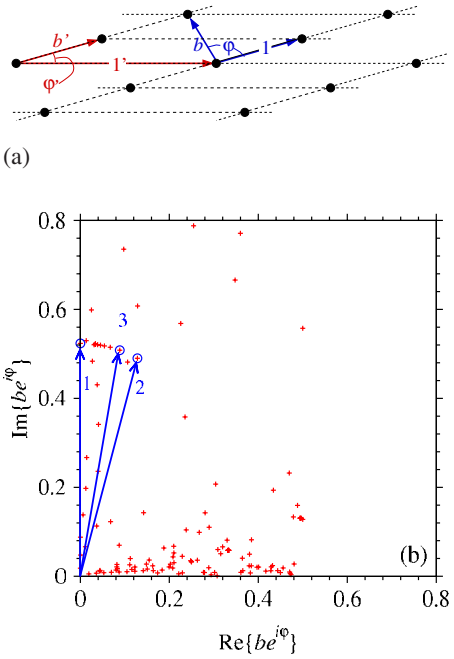

FIG. 4. (Color online) (a) The values b' and φ' derived directly from Eq. (9) define a lattice which can be represented by a rescaling and the reduced variables b and φ. (b) The unit cells of the reduced, zero-energy lattices are defined by the unit vector in the x direction and a basis vector to any one of the points shown. The first 100 reduced basis vectors (with one of the basis vectors scaled to unit amplitude and directed along the x axis) are shown. The lattice basis vectors corresponding to the three circled roots in Fig. 3(a) are indicated.

computed numerically to 24 digit precision using the NSolve function in Mathematica. This function employs the Jenkins-Traub algorithm [11] which is globally convergent and gives all complex roots of a finite-order polynomial such as Eq. (10). These roots, along with their inverses (which are also roots) are shown in Fig. 3.

Although the zeros of $|S(\xi)|$ yield associated lattice parameters b, φ via Eq. (9), the values $\{b, \varphi\}$ found from the roots ξ_i do not uniquely determine the geometry of a unit cell. Therefore, basis vector reduction is performed to obtain the smallest possible unit cell that can represent an identical lattice for every set $\{b, \varphi\}$. The reduced vectors are found by first identifying the vector with a minimum distance between $nbe^{i\varphi}$ and the unit lattice vector. This difference vector is $1 - n^* be^{i\varphi}$, where n^* is the nearest integer of the value n that minimizes $1 - n^* be^{i\varphi}$. If the magnitude of the distance vector is less than unity, we rescale both $1 - n^* be^{i\varphi}$ and $be^{i\varphi}$ such that the longest vector is reduced to the new unit basis vector. The two new basis vectors are

$$\frac{be^{i\varphi}}{\max\{|1 - n^* be^{i\varphi}|, b\}}, \quad \frac{1 - n^* be^{i\varphi}}{\max\{|1 - n^* be^{i\varphi}|, b\}}. \quad (11)$$

The lattice vector reduction is illustrated in Fig. 4(a). After rotating the longer basis vector in (11) onto the real axis, the remaining basis vectors are plotted in Fig. 4(b), revealing the unit cell geometries. The pattern of roots [Fig. 3(a)] and the

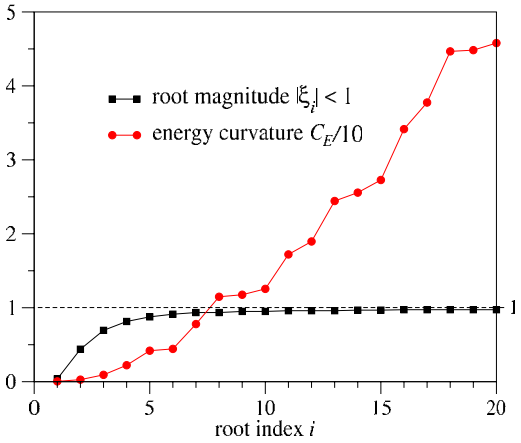

FIG. 5. (Color online) The curvature of the energy $C_E(i)(/10)$ at the energy minima defined by ξ_i. The root index i orders the roots by increasing magnitude. The curvature is shown to increase as the magnitude of the associated root $|\xi_i|<1$ increases.

corresponding lattice structures [Fig. 4(b)] appear to follow a complex pattern. For concreteness, the lattice vectors for the two real roots (labeled "1" and "2") at $\xi=0.0372768$ and $\xi=-0.439293$ are defined by $\{b,\varphi\}=\{0.523522,\pi/2\}$ and $\{b,\varphi\}=\{0.256642,1.826885\}$, respectively. The basis vectors corresponding to these roots make angles of 90° and 75.33° with respect to the x axis, respectively, and are shown in Fig. 3(b). Similarly, we consider the lowest magnitude complex root $\xi=-0.34687320+0.60086689i$ has a corresponding reduced basis vector indicated by "3" in Fig. 4(b). This vector makes a 80.106° angle with respect to the x axis.

We briefly discuss the effects of noncircular lattice inclusions. For a perfect lattice of inclusions with equal ellipticity, the minimum-energy orientation angle θ_0 is found from the conditions

$$\left(\frac{\partial E_N}{\partial \theta_j}\right)_{\theta_j=\theta_0}=0 \quad \text{and} \quad \left(\frac{\partial^2 E_N}{\partial \theta_j^2}\right)_{\theta_j=\theta_0}>0, \tag{12}$$

which for the convention $\varepsilon>0$ requires

$$\theta_0=\frac{1}{2}(\pi-\Phi) \quad \text{and} \quad \Phi\equiv\arg[S(\xi)]. \tag{13}$$

This minimum-energy orientation is associated with the lattice constants found by minimizing the energy

$$E=64\pi^4 E_0\left(\frac{r_0}{a}\right)^4 N\left[|S(\xi)|-\varepsilon\left(\frac{a}{4\pi r_0}\right)^2\right]^2 \tag{14}$$

with respect to ξ. The lattice constants of elliptical inclusions are now determined by $|S(\xi)|=\varepsilon(a/4\pi r_0)^2$. Small ellipticities ε can alter the lattice structure since the basis vectors are now found from roots of the shifted function $|S(\xi)|-\varepsilon(\frac{a}{4\pi r_0})^2$. This shift of $\varepsilon(a/4\pi r_0)^2$ may be sizable. When ellipticity is considered, the degeneracy is expanded and a circle of values ξ appears about each ξ_i that minimized the energy of circular inclusions.

Finally, even though all minimum-energy states have zero membrane bending energy, the curvature of the energies at the roots ξ_i varies significantly. For a lattice of circular inclusions, the total curvature $C_E(i)$ of the energy at the minima is found from

$$C_E(i)=\left.\frac{\partial^2|S(\xi)|^2}{\partial\xi\,\partial\,\xi^*}\right|_{\xi=\xi_i}=\left|\left.\frac{\partial S(\xi)}{\partial\xi}\right|_{\xi=\xi_i}\right|^2=\left|\sum_{p=1}^{\infty}\frac{p\xi_i^p}{(\xi_i^p-1)^2}\right|^2 \tag{15}$$

and are plotted in Fig. 5 as a function of the root index i for increasing $|\xi_i|$, which is also plotted. The results show that the energy curvature near the minima defined by the larger root indices is higher, indicating that these higher index lattices are more rigid against nondilational structural deformations.

IV. DISCUSSION AND CONCLUSIONS

We have investigated the structures that arise when inclusions interact via bending-mediated forces. In an infinite, doubly periodic system, the membrane bending-mediated multibody interaction [Eq. (3)] previously found [1] gives rise to an unexpected infinitely degenerate ground state. This ground state is realized by nontrivial lattices. This feature is not only qualitatively different from the triangular lattice expected from compression of pairwise interacting particles in two dimensions, but also contrasts with the nearly triangular local structures seen within finite clusters of inclusions [1].

Since the zero energies of the degenerate structures are invariant to dilatations, additional pairwise interaction energies and external chemical potentials would be required to set the overall particle density. However, lattices with larger root index (roots ξ_i with larger magnitude) have larger energy curvatures C_E and are more rigid with respect to shearing deformations. Moreover, an infinite system with the same lattice structure [corresponding to the same root of $S(\xi)$] may have a positive energy if the lattice spacing varies across the sample. Therefore, thermal excitations can lead to variations in lattice spacing (with the same lattice structure) or with varying lattices. Analyses of the lowest energy excitations would require summation of the full energy since the interactions are long ranged and multibodied. This is in contrast to Fourier-type decompositions of thermal excitations in pairwise interacting lattices. This nonlocal aspect is suggested by the fact that the local lattice structure in minimum-energy finite clusters is triangular or square [1], while the zero-energy structures of a zero-energy infinite lattice are much more complicated.

Although thermal effects are difficult to analyze in this model compared to pairwise interacting particle systems, where interactions are short ranged and deformations can be decomposed, the thermalization of the orientational order of elliptical inclusions can be straightforwardly analyzed. Upon integrating out inclusion angles θ_j using a Boltzmann distribution over the energy in Eq. (8), each inclusion is rendered effectively circular and the infinitely degenerate lattices are preserved, but with a slight renormalization in the total interaction energy [15].

Finally, membrane tension imposes a cutoff in membrane bending, which can render the interactions short ranged and pairwise additive. In systems where a surface tension σ is present, the appropriate Helfrich energy takes the form

$$\mathcal{H}_{\mathrm{mem}} = \frac{\kappa}{2}\oint\!\!\!\oint K^2(\mathbf{S})d\mathbf{S} + \sigma\oint\!\!\!\oint d\mathbf{S}. \tag{16}$$

In this case, the multibody interactions will be short range, extending over a length $\ell = \sqrt{\kappa/\sigma}$ [18], and we expect the collective properties for the inclusions to be qualitatively different for density variations with wavelength greater than ℓ. We expect a crossover from multibody interactions to pairwise interactions as ℓ is tuned via an applied tension σ. Surface tension in the membrane would then destroy the infinitely degenerate energy surface. A confining external chemical potential in this case would result in a triangular lattice of particles.

ACKNOWLEDGMENTS

T.C. was supported by grants from the NSF (Grant No. DMS-0349195) and the NIH (Grant No. K25 AI41935). K.S.K. acknowledges support from DOE-UC CCB Grant No. W-7405-ENG-48.

[1] K. S. Kim, J. C. Neu, and G. Oster, Biophys. J. **75**, 2274 (1998).
[2] B. Alberts, A. Johnson, J. Lewis, M. Raff, K. Roberts, and P. Walter, *Molecular Biology of the Cell*, 4th ed. (Garland, New York, 2002).
[3] D. Bray, M. D. Levin, and C. J. Morton-Firth, Nature (London) **393**, 85 (1998).
[4] C. Guo and H. Levine, Biophys. J. **77**, 2358 (1999).
[5] M. M. Müller, M. Deserno, and J. Guven, Phys. Rev. E **72**, 061407 (2005).
[6] M. Grabe, J. Neu, G. Oster, and P. Nollert, Biophys. J. **84**, 854 (2003).
[7] *Theory of Elasticity*, edited by L. D. Landau and E. M. Lifshitz (Pergamon, New York, 1981).
[8] A. Iglič, H. Hägerstrand, P. Veranič, A. Plemenitaš, and V. Kralj-Iglič, J. Theor. Biol. **240**, 368 (2006).
[9] U. Seifert, Phys. Rev. Lett. **70**, 1335 (1993).
[10] K. S. Kim, J. C. Neu, and G. Oster, Phys. Rev. E **61**, 4281 (2000).
[11] M. A. Jenkins and J. F. Traub, SIAM (Soc. Ind. Appl. Math.) J. Numer. Anal. **7**, 545 (1970).
[12] P. G. Dommersnes and J. B. Fournier, Eur. Phys. J. B **12**, 9 (1999).
[13] P. G. Dommersnes and J. B. Fournier, Europhys. Lett. **46**, 256 (1999).
[14] L. Hasler, J. B. Heymann, A. Engel, J. Kistler, and T. Walz, J. Struct. Biol. **121**, 162 (1998).
[15] T. Chou, K. S. Kim, and G. Oster, Biophys. J. **80**, 1075 (2001).
[16] P. B. Canham, J. Theor. Biol. **26**, 61 (1970); W. Helfrich, Z. Naturforsch. [C] **28**, 693 (1973).
[17] *Methods of Theoretical Physics, Part I*, edited by P. M. Morse and H. Feshbach (McGraw-Hill, New York, 1953).
[18] T. R. Weikl, M. M. Kozlov, and W. Helfrich, Phys. Rev. E **57**, 6988 (1998).